Geochemistry Geophysics Geosystems G3

Article
Volume 13, Number 8
3 August 2012
Q08Z47, doi:10.1029/2012GC004195
ISSN: 1525-2027

Published by AGU and the Geochemical Society

Pyrrhotite as a tracer for denudation of the Taiwan orogen

Chorng-Shern Horng, Chih-An Huh, Kuo-Hang Chen, and Chun-Hung Lin
Institute of Earth Sciences, Academia Sinica, PO Box 1-55, Nankang, Taipei 11529, Taiwan (cshorng@earth.sinica.edu.tw)

Kai-Shuan Shea
Central Geological Survey, Ministry of Economic Affairs, PO Box 968, Taipei 23568, Taiwan

Kan-Hsi Hsiung
Institute of Oceanography, National Taiwan University, Taipei 10617, Taiwan

[1] The use of pyrrhotite as an index mineral to delineate metamorphic isograds has long been proposed. However, details of the occurrence of pyrrhotite in different metamorphic facies and its implications have rarely been explored. Here, by simple characterization of magnetic properties and mineral identification, we demonstrate that pyrrhotite is widely distributed in low-grade metamorphic terranes of Taiwan's Central Range and in sediments derived therefrom. By coupling the distribution of pyrrhotite in rocks with that in dated sediment strata, we have studied the denudation history of Taiwan's orogen from a source-to-sink perspective. We suggest that pyrrhotite is a potential tracer for studying surface processes in orogens with high denudation rates similar to that in Taiwan.

Components: 4600 words, 6 figures.

Keywords: denudation; magnetic tracers; orogenic belt; pyrrhotite; regional metamorphism; surface processes.

Index Terms: 1165 Geochronology: Sedimentary geochronology; 1512 Geomagnetism and Paleomagnetism: Environmental magnetism; 1520 Geomagnetism and Paleomagnetism: Magnetostratigraphy; 1540 Geomagnetism and Paleomagnetism: Rock and mineral magnetism; 1862 Hydrology: Sediment transport (4558).

Received 23 April 2012; **Revised** 3 July 2012; **Accepted** 6 July 2012; **Published** 3 August 2012.

Horng, C.-S., C.-A. Huh, K.-H. Chen, C.-H. Lin, K.-S. Shea, and K.-H. Hsiung (2012), Pyrrhotite as a tracer for denudation of the Taiwan orogen, *Geochem. Geophys. Geosyst.*, *13*, Q08Z47, doi:10.1029/2012GC004195.

Theme: Magnetism From Atomic to Planetary Scales: Physical Principles and Interdisciplinary Applications in Geosciences and Planetary Sciences

1. Introduction

[2] Collisions at plate boundaries lead to deformation of the Earth's crust and to creation of orogenic belts. In addition to endogenetic processes such as plate tectonics and orogeny, exogenetic processes like weathering, erosion, mass wasting and sedimentation modify the landscape toward a more subdued and stable state. Fluvial systems play an important role in shaping the Earth's surface by transporting weathering products from their source regions to inland or offshore basins for temporary storage or long-term burial. To maintain isostasy, denudation must keep pace with bedrock uplift.

This explains why, on a global basis, sediments disgorged to deep oceans are mainly carried by rivers that drain the world's steepest orogens [*Ludwig and Probst*, 1998]. Previous studies have indicated that about 70% of the global fluvial sediment discharge is from orogens in southern Asia and mountainous islands that fringe the Pacific and Indian Oceans [*Milliman and Meade*, 1983]. This is due to a complex interplay between active tectonism, steep topography, heavy rainfall, and intense anthropogenic landscape modification in these regions [*Griffiths*, 1979; *Milliman and Syvitski*, 1992; *Dadson et al.*, 2003].

[3] To investigate source-to-sink transport of sediments on various temporal and spatial scales, various geochemical or mineralogical tracers have been employed. Although environmental magnetism has been increasingly applied to address such issues [e.g., *Evans and Heller*, 2003], magnetic minerals derived from orogenic belts remain poorly studied. Since magnetite (Fe_3O_4) is in general the most abundant magnetic mineral in the Earth's crust, it has been thought to be widespread in orogenic belts as well. Using magnetic properties and mineral identification, we report here that monoclinic pyrrhotite (Fe_7S_8) is even more common than magnetite in Taiwan's orogen, which has been exhumed episodically during the Plio-Pleistocene. Following rapid transport by rivers, detrital pyrrhotite that has been eroded from mountain ranges can be preserved in marginal marine sedimentary basins. Therefore, besides its utility as a tracer for source-to-sink transport of sediments [*Horng and Roberts*, 2006; *Horng and Huh*, 2011], pyrrhotite can also be used to reconstruct the exhumation and denudation history of Taiwan's orogen and, by extension, similar orogens with high denudation rates.

2. Tectonic Setting and Geology of Taiwan

[4] Taiwan is located between the Eurasian Plate and the Philippine Sea Plate (inset in Figure 1). Oblique collision between these plates has led to the buildup of Taiwan's mountain ranges since the Pliocene [*Ho*, 1975]. Foreland, forearc, and back-arc basins have also developed in the Taiwan Strait, the Huatung Basin, and the Southern Okinawa Trough, respectively. Geologically, Taiwan is divided by three major faults into four tectonostratigraphic provinces, which are, from the east to the west, the Coastal Range, the Central Range, the Western Foothills and the Coastal Plain (Figure 1). The Coastal Range is an accreted portion of the northern Luzon Arc. It consists of andesitic lavas, pyroclastics and a thick Plio-Pleistocene sedimentary succession in an ancient forearc basin (Figure 2a). The Central Range has been exhumed since the Plio-Pleistocene to form the backbone of the island and it can be divided into the eastern and western subprovinces. The eastern part consists of a variety of pre-Tertiary basement rocks including schists, marbles, amphibolites, metadiabases, and gneisses (Figure 2a). During the orogeny, this rock complex underwent retrograde metamorphism from amphibolite facies in the Mesozoic to greenschist facies in the Plio-Pleistocene. The western part of the Central Range is a highly deformed slate belt that lies unconformably over the basement complex. This belt was formed by regional metamorphism during the Plio-Pleistocene, which transformed a thick sequence of Tertiary marine sediments to rocks of subgreenschist facies, including argillites, slates, phyllites, and quartzites. Using illite crystallinity as an index of metamorphic grade, *Chen and Wang* [1995] classified the slate belt into epizone and anchizone, which correspond, respectively, to formations of Eocene-Oligocene and Oligocene-Miocene age (Figure 2a). The Western Foothills consist of unmetamorphosed Oligocene to Pleistocene siliciclastic sediments that were uplifted and deformed into a series of imbricated thrust sheets (Figure 2a). The Coastal Plain is covered by alluvium and terrace deposits that are underlain by Plio-Pleistocene marine sediments in an ancient foreland basin. Last, Pleistocene volcanism produced the Tatun and the Chilung volcanic groups (V_T and V_C in Figure 2a) in northern Taiwan.

3. Surface Processes in the Taiwan Orogen

[5] The geomorphology of Taiwan (Figure 1) reflects a long-term interaction between orogenic and surface processes. Located in an active tectonic setting with tropical to subtropical climate and ~4 typhoons per year, Taiwan has high denudation rates (3–6 mm/yr) in response to its rapid uplift since the Plio-Pleistocene [*Li*, 1976]. Despite the fact that Taiwan's rivers are short (<190 km) and drainage basins are small (<3300 km^2), their sediment yields are among the highest in the world [*Milliman and Syvitski*, 1992]. The total sediment load of Taiwan's rivers is ~380 Mt/yr, which produces 1.9% of global fluvial sediment discharge from only 0.024% of the Earth's subaerial surface [*Dadson et al.*, 2003]. The Central Range divides

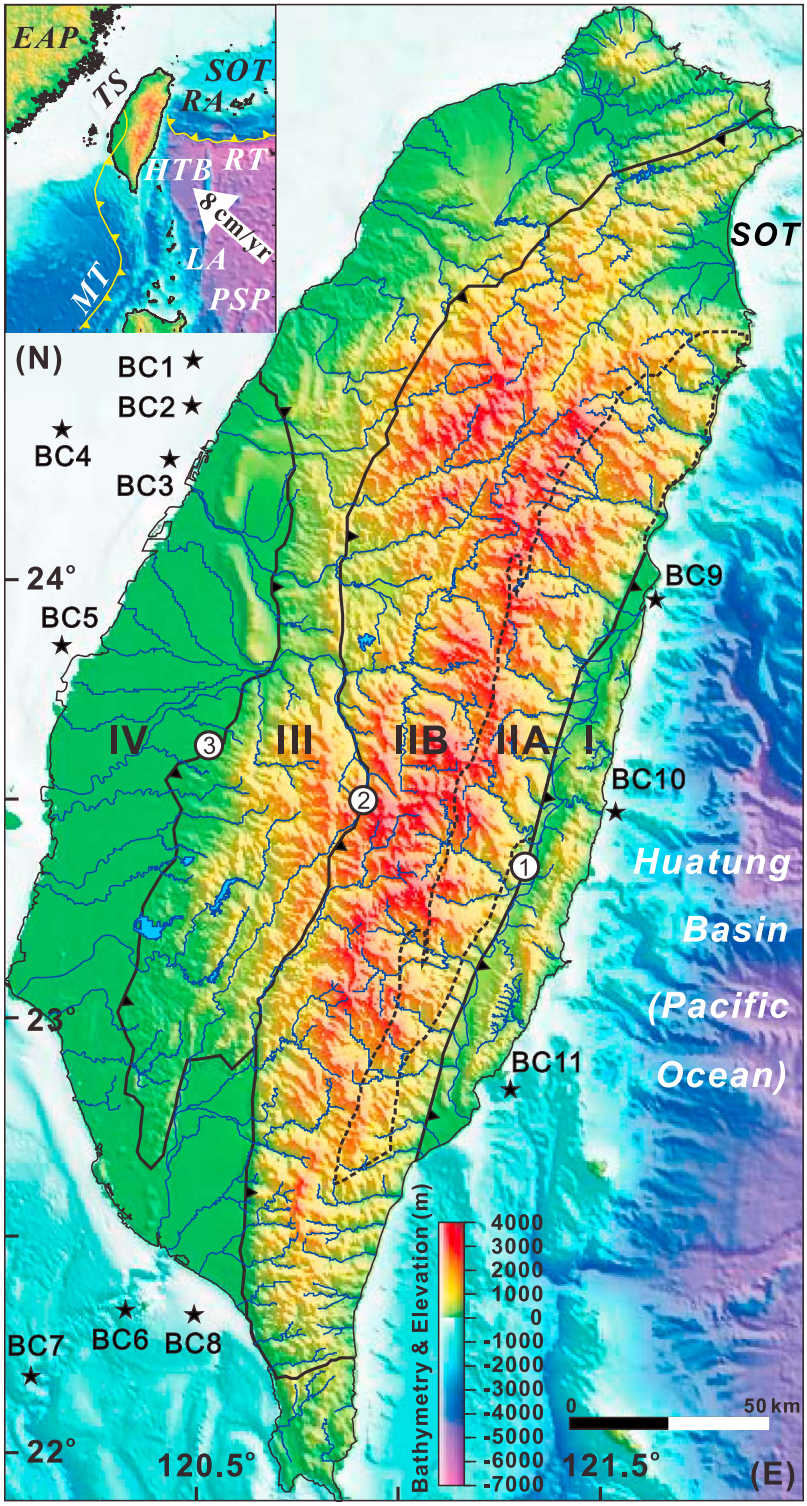

Figure 1. Topographic map of Taiwan and bathymetry of the surrounding seafloor. The upper left-hand inset is a sketch of the tectonic setting around Taiwan (PSP/EAP: Philippine Sea/Eurasian Plate; MT/RT: Manila/Ryukyu Trench; LA/RA: Luzon/Ryukyu Arc; SOT: Southern Okinawa Trough; HTB: Huatung Basin; TS: Taiwan Strait). Taiwan is demarcated by three tectonic suture lines (1: Longitudinal Valley; 2: Chuchih Fault; 3: Chukou Fault) into four major geological provinces (I: Coastal Range; IIA and IIB: Eastern and Western Central Ranges; III: Western Foothills; IV: Coastal Plain). Stars around Taiwan indicate sites of box-cored sediments (BC1-BC11) used for this study.

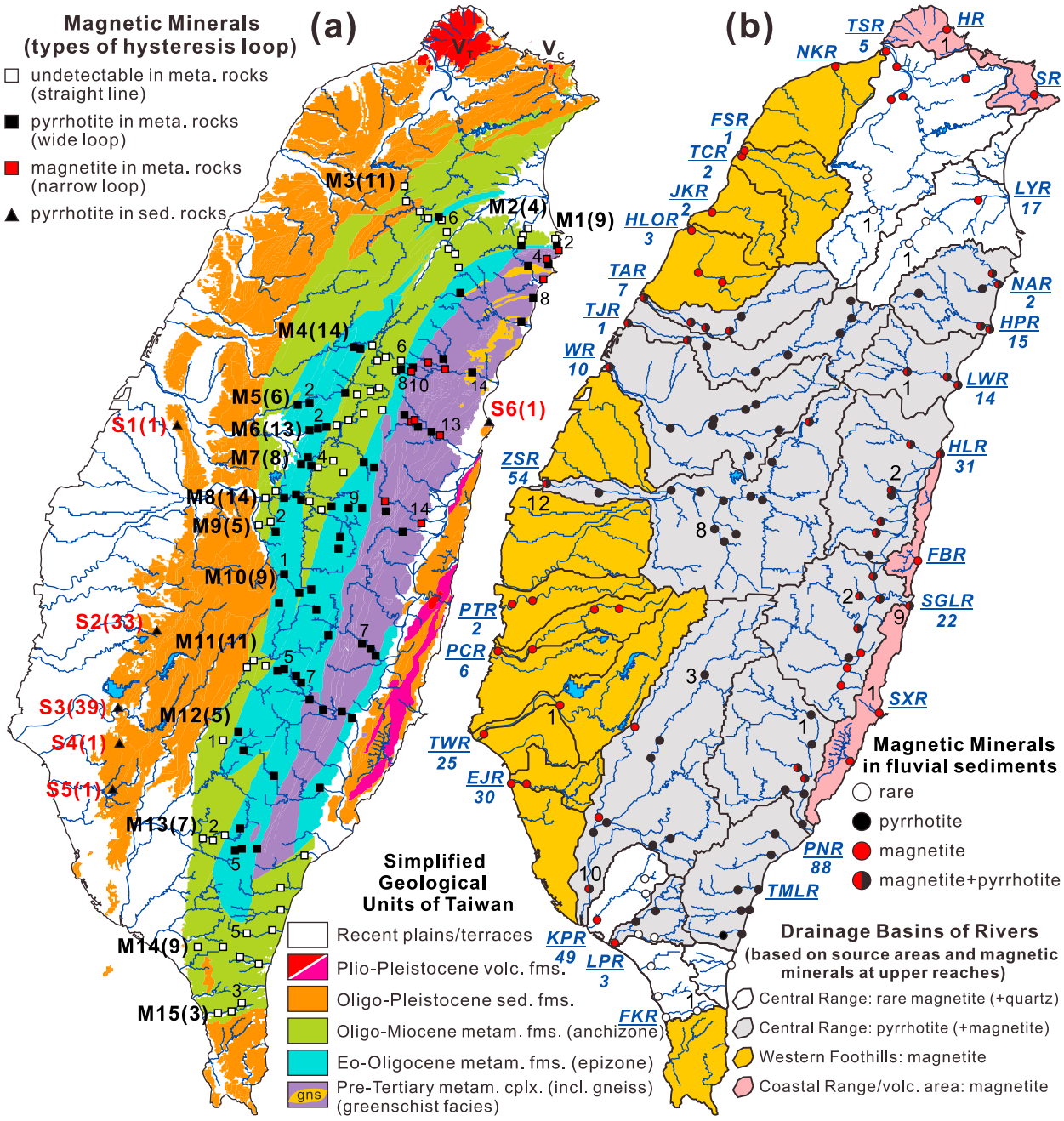

Figure 2. (a) A simplified geological map of Taiwan with occurrences of magnetic minerals in metamorphic rocks indicated along 15 transects in the Central Range (M1-M15: squares) and pyrrhotite in 6 Plio-Pleistocene sedimentary sections (S1-S6: triangles). Numbers in parentheses indicate the total number of specimens collected from each transect or section. Numbers next to the squares correspond to the labels for hysteresis loops, SEM images and XRD spectra shown in Figure 3. (b) Map of Taiwan's drainage basins and the distribution of magnetic minerals in fluvial sediments (circles). Numbers next to the circles correspond to those for XRD spectra shown in Figure 4. For brevity, names of rivers are acronymed (for details of Taiwan's rivers, refer to auxiliary material). The numbers under the acronyms represent each river's sediment loads (in Mt/yr [*Dadson et al.*, 2003]).

Taiwan's major rivers into two sectors (Figures 1 and 2). Included in the western sector are three longest rivers, namely the Zhuoshui, the Kaoping and the Tamshui Rivers (ZSR, KPR, and TSR in Figure 2b), which flow into the Taiwan Strait. In the eastern sector are generally shorter rivers that flow over steeper gradients toward the Pacific Ocean, such as the Hualien (HLR), the Siouguluan

(SGLR) and the Peinan Rivers (PNR), which empty into the Huatung Basin, and the Lanyang River (LYR), which discharges toward the Southern Okinawa Trough (Figure 2b). In contrast, rivers that originate either from the sedimentary Western Foothills or volcanic-dominated regions generally have lower sediment loads (<6 Mt/yr), with the exception of the Tsengwen and the Erhjen Rivers (TWR and EJR in Figure 2b), which pass through poorly consolidated Plio-Pleistocene mudstones. Generally speaking, denudation of the Central Range accounts for much of the sediment load of Taiwan's rivers.

4. Sampling and Methods

[6] Since the first report of the occurrence of pyrrhotite in the southern Central Range [*Horng and Roberts*, 2006], the distribution of this magnetic mineral in and around the contiguous orogenic belt has remained unclear. In this study, we conducted a comprehensive survey and intensive sampling of metamorphic rocks of various grades along 15 transects across the Central Range (labeled M1-M15 in Figure 2a). We also collected fluvial sediments from riverbanks (Figure 2b), box-cored sediments off the mouths of major rivers (BC1-BC11 in Figure 1), and sedimentary rocks from Plio-Pleistocene sections in the Western Foothills and the Coastal Range (S1-S6 in Figure 2a). Information for all samples can be found in the auxiliary material.[1]

[7] To characterize the magnetic properties of metamorphic rocks, magnetic hysteresis loops were measured on small samples (300–500 mg) using a Princeton Measurements Corporation vibrating sample magnetometer. Magnetic fields from +0.5 T to −0.5 T were applied to the samples. Magnetic minerals were extracted from all fluvial and marine sediments, and from some of the metamorphic and sedimentary rocks. These rocks were crushed and gently ground into a fine powder, and suspended in water. Magnetic minerals were extracted using a rare earth magnet housed in a plastic sheath. The other samples (fluvial and box-cored sediments) were simply mixed with water (making a slurry for the sediment samples) and the magnetic minerals were extracted as above. Then, X-ray diffraction (XRD) analysis was made using a Rikagu Miniflex table top unit with Cu-Kα radiation. Scans were run from 4° to 80° of 2θ. Results are presented after subtraction of the background trend. Direct observations of magnetic minerals in polished thin sections of metamorphic and sedimentary rocks and in the magnetic extracts were made using a JEOL JSM-6360LV scanning electron microscope (SEM) operated at 15 keV with 18 nA acceleration voltage. Mineral compositions were determined using an Oxford Instruments Ltd INCA-300 X-ray energy dispersive spectrometer (EDS) attached to the SEM. To establish biostratigraphy, smear slides for calcareous nannofossil observations under optical microscope were prepared on sedimentary rocks from the S2 and S3 sections.

[1]Auxiliary materials are available in the HTML. doi:10.1029/2012GC004195.

5. Magnetic Minerals and Properties in Metamorphic Rocks of Taiwan Orogen

[8] Magnetic hysteresis loops determined for the metamorphic rocks can be classified into three types: straight lines, wide loops, and narrow loops (Figures 3a, 3b and 3c). The straight-line type is dominated by paramagnetic minerals and reveals an absence of ferrimagnetic minerals. In contrast, the wide and narrow loops indicate the presence of ferrimagnetic phases with higher (10–35 mT) and lower (<5 mT) coercivities, respectively. SEM and EDS analyses of opaque minerals on thin sections further indicate that non-magnetic framboidal pyrite crystals are common in rocks of the straight-line type, while platy pyrrhotite and granular magnetite are, respectively, the dominant magnetic minerals in samples from which the wide and narrow hysteresis loops are obtained (Figures 3d and 3e). XRD analysis of the magnetic extracts confirms these observations (Figure 3f). When the hysteresis results are summarized against the geological backdrop presented in Figure 2a, we found that the straight-line type of hysteresis loop is confined to the anchizone, while the wide-loop type occurs mainly in the epizone and extends to the pre-Tertiary greenschist facies. Previous studies have claimed that pyrrhotite is transformed from pyrite by increasing metamorphism and that the incipient occurrence of pyrrhotite in a sequence of metamorphic rocks can be used to identify a new metamorphic isograd [e.g., *Carpenter*, 1974; *Rochette*, 1987]. In Figure 3d, small framboidal pyrite grains appear to have coalesced to form a large pyrrhotite crystal, which lends strong support to this conclusion. Using isotopic composition and Raman spectroscopy of carbonaceous material, respectively, *Yui* [2005] and *Beyssac et al.* [2007] estimated that metamorphic rocks in Taiwan with grades higher than anchizone were formed at temperatures ranging from ~300°C to ~500°C, suggesting that the incipient temperature of pyrrhotite

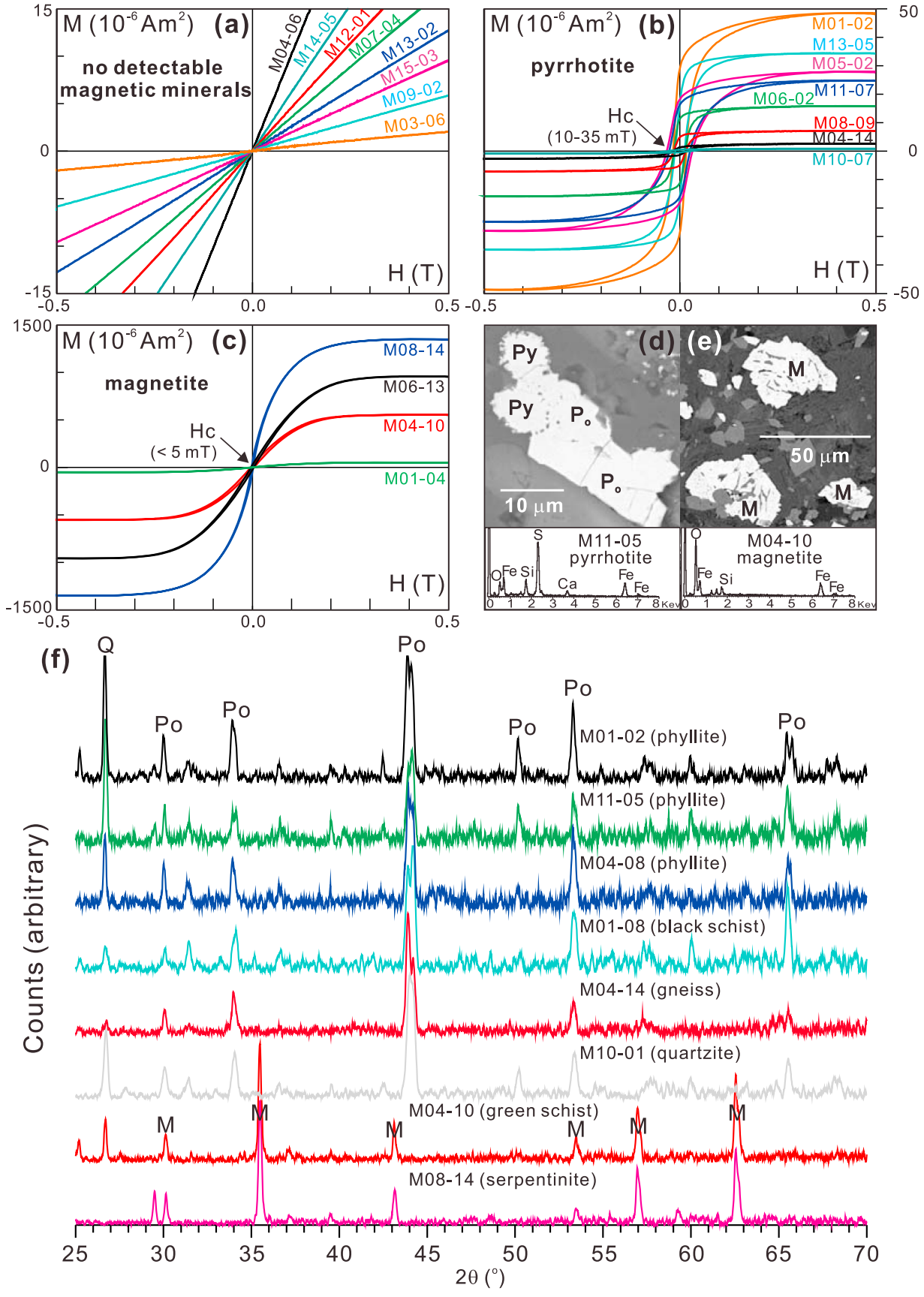
M (10-6Am2) (a)
no detectable magnetic minerals
M04-06
M14-05
M12-01
M07-04
M13-02
M15-03
M09-02
M03-06
H (T)
M (10-6Am2) (b)
pyrrhotite
Hc (10-35 mT)
M01-02
M13-05
M05-02
M11-07
M06-02
M08-09
M04-14
M10-07
H (T)
M (10-6Am2) (c)
magnetite
Hc (< 5 mT)
M08-14
M06-13
M04-10
M01-04
H (T)
(d)
Py
Py
Po
Po
10 μm
(e)
M
M
M
50 μm
M11-05 pyrrhotite
M04-10 magnetite
(f)
Q
Po
Po
Po
Po
Po
M01-02 (phyllite)
M11-05 (phyllite)
M04-08 (phyllite)
M01-08 (black schist)
M04-14 (gneiss)
M10-01 (quartzite)
M04-10 (green schist)
M08-14 (serpentinite)
Counts (arbitrary)
2θ (°)

Figure 3

formation was near 300°C. These results are consistent with the study of *Itaya* [1975], who proposed that the Sanbagawa pelitic pyrrhotite-bearing schists in Central Shikoku of Japan were metamorphosed at temperatures above 310°C.

[9] Rocks with narrow hysteresis loops are all from green-colored rocks of the greenschist facies (e.g., green schist and serpentinite; Figure 3f), which are mainly distributed in the northeastern Central Range (Figure 2a). This indicates that magnetite-bearing metamorphic rocks originated from mafic protoliths. By contrast, pyrrhotite exists in a wide variety of meta-sedimentary rocks, including phyllites, quartzites, black schists, and gneisses (Figure 3f). Overall, pyrrhotite is more common than magnetite in Taiwan's Central Range (Figure 2a).

6. Pyrrhotite as a Tracer for Sediments From Source to Sink

[10] XRD results for magnetic mineral extracts from all fluvial sediments are summarized in Figure 2b, with representative X-ray diffractograms illustrated in Figure 4. Magnetite is the only magnetic mineral detected in fluvial sediments from the Western Foothills (TWR-1), the Coastal Range (SXR-1), and the northern tip of Taiwan (HR-1) (Figure 4a). This suggests that magnetite is a primary magnetic mineral in Taiwan's volcanic and sedimentary terranes. As for fluvial sediments sourced from metamorphic terranes of the Central Range, their magnetic mineral components are largely dictated by the lithology in the upper reaches of the respective rivers and can be divided into three types. The first type, which is characterized by a trace amount or total absence of magnetite, is found in rivers that drain the anchizone of the slate belt such as the Tamshui, the Lanyan and the Fengkang Rivers (TSR-1, LYR-1 and FKR-1; Figures 2 and 4a). The second type, which is dominated by pyrrhotite, is typical of sediments transported by mountainous rivers from the epizone of the slate belt (ZSR-8, KPR-3 and PNR-1; Figures 2 and 4b). The third type, in which magnetite coexists with pyrrhotite or where magnetite dominates over pyrrhotite, is typical of sediments carried by eastward flowing rivers (e.g., the Liwu, the Hualien and the Siouguluan Rivers; LWR-1, HLR-2 and SGLR-2; Figures 2 and 4b), which drain not only the epizone (or complex) but also magnetite-bearing volcanic rocks of the Coastal Range. Pyrrhotite eroded from metamorphic terranes can be preserved in estuarine sediments (ZSR-12, KPR-10, and SGLR-9; Figures 2b and 4c) or in modern foreland/forearc basins (BC4, BC7 and BC10; Figures 1 and 4c), which suggests rapid transport and burial of fluvial sediments. Although pyrrhotite is derived from the upper reaches of mountainous rivers, it can be mixed with magnetite derived from volcanic and sedimentary terranes in the lower reaches of some rivers (Figure 2b). Pyrrhotite is also found in sediments of the Ta-an River (TAR; Figure 2b), which suggests that TAR must have drained an epizone in its upper reaches. The lack of such an area in all published geological maps (e.g., Figure 2a) suggests that more detailed geological surveying near the TAR headwaters is warranted.

[11] In summary, pyrrhotite eroded from the metamorphic terranes of Taiwan's Central Range occurs commonly in fluvial and offshore sediments. As such, it can be used as a diagnostic tracer for sediment transport from source to sink [*Horng and Huh*, 2011].

7. Exhumation and Denudation Records of Taiwan's Central Range

[12] As *Horng et al.* [1992,1998] reported previously, pyrrhotite was also found in the Plio-Pleistocene sedimentary strata of Taiwan (e.g., in Sections S1-S6; Figures 2a and 4d). The detrital morphology of pyrrhotite grains (see Figures 4e and 4f) suggests that they were eroded from the Central Range. Among Sections S1 through S6, S2 and S3 have extraordinarily thick strata that constitute a complete Plio-Pleistocene sedimentary succession in southwestern Taiwan. Thus, the occurrence of detrital pyrrhotite in these two sections may shed light on the denudation history of the Central Range.

[13] Figure 5 shows sites along Sections S2 and S3 where samples were collected for detailed chronological and magnetic mineral studies in this and previous works [*Chen et al.*, 2001]. Three datum events of calcareous nannofossils were identified in these sections: the last occurrence datum of

Figure 3. (a–c) Three types of characteristic hysteresis loops for different magnetic mineral compositions in metamorphic rocks from Taiwan's Central Range. (d–e) SEM images of granular magnetite (M) and platy pyrrhotite (Po) transformed from framboidal pyrite (Py). (f) Representative X-ray diffractograms of magnetic extracts from various types of metamorphic rocks with characteristic peaks for pyrrhotite, magnetite, and quartz (Q). Samples M04–10 and M08–14 contain magnetite only, while the rest contain pyrrhotite.

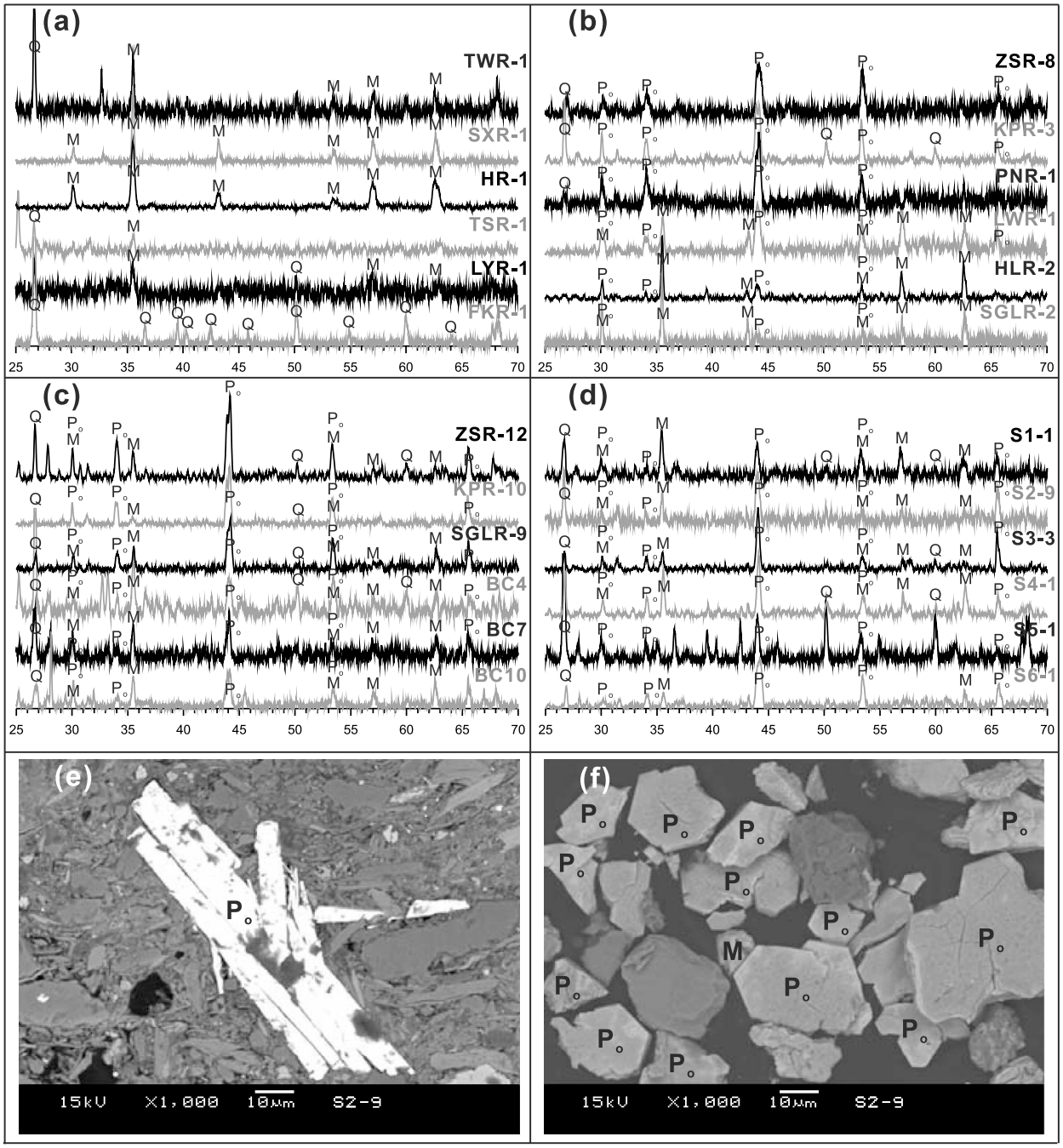

Figure 4. (a–d) Representative X-ray diffractograms for magnetic extracts from fluvial sediments (from TWR-1 to SGLR-9), marine sediments (BC4, BC7, and BC10) and sedimentary rocks (from S1–1 to S6–1). Labels for the vertical and horizontal axes are counts (arbitrary) and 2θ, respectively. Po: pyrrhotite; M: magnetite; Q: quartz. SEM images of (e) pyrrhotite in a thin-sectioned specimen from the S2 section (S2–9), showing a detrital texture and (f) magnetic grains extracted from the same specimen, showing a hexagonal-like outline of pyrrhotite particles. It should be noted that according to their magnetic characters and double X-ray diffraction peaks at ~44° (2θ) as shown in Figure 3f [*Graham*, 1969], pyrrhotite discussed here is ferrimagnetic monoclinic pyrrhotite instead of paramagnetic hexagonal pyrrhotite, although its morphology looks hexagonal-like [see also *Horng et al.*, 1998; *Horng and Roberts*, 2006; *Horng and Huh*, 2011].

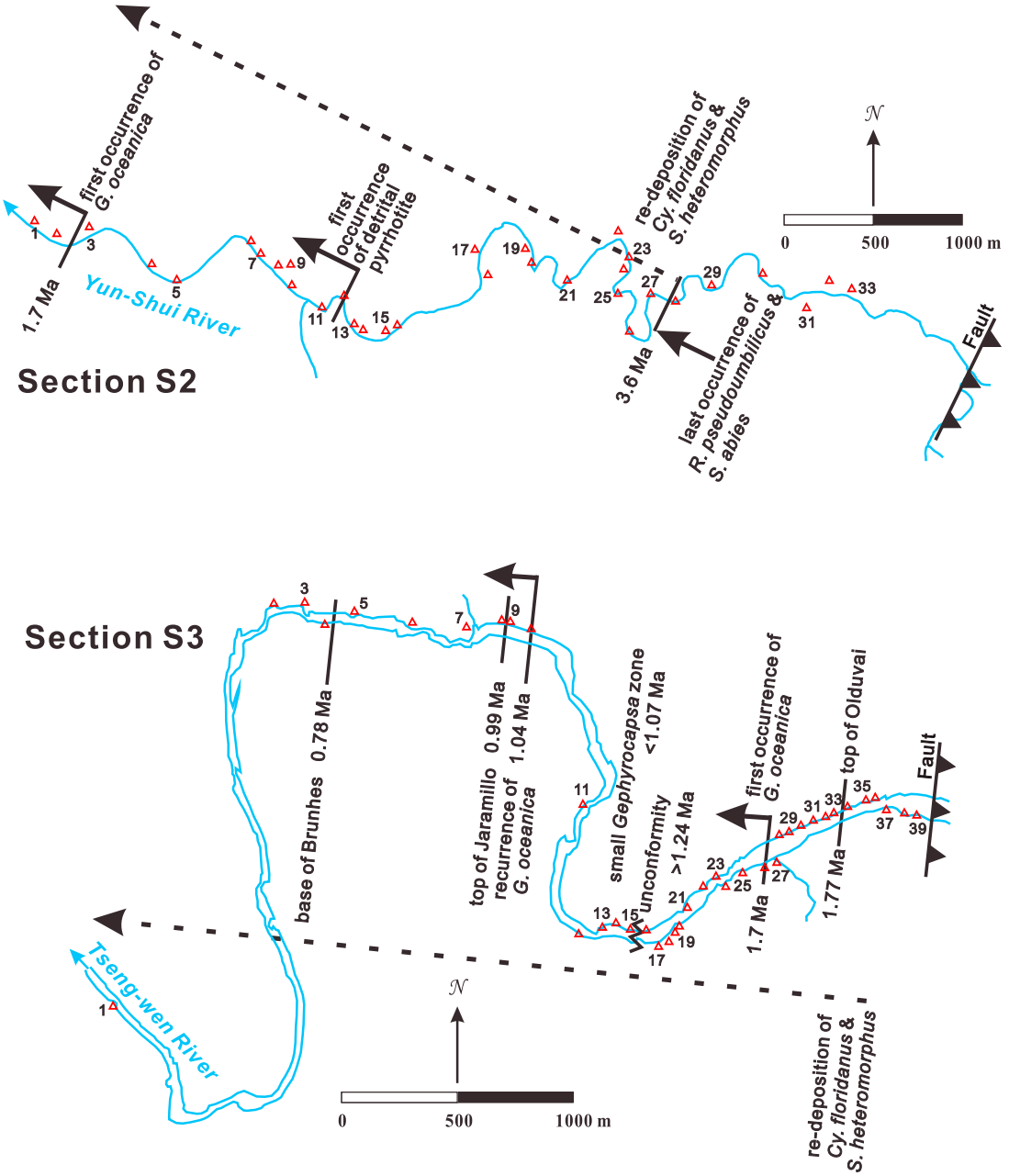

Figure 5. Map showing sampling sites (Δ) for magnetic mineral analysis and chronological study of two sedimentary sections (S2 and S3) in southwestern Taiwan. The first occurrence of detrital pyrrhotite is located at site 12 of Section S2. An unconformity between site 15 and site 16 in Section S3 marks abrupt discontinuities of lithology, magnetic mineral composition, nannofossils, and geomagnetic polarities. On the eastern side of the discontinuity, nannofossil species *Gephyrocapsa oceanica* in medium to large-sizes (3.5–5.5 μm) can be recognized, indicating that the age of strata is older than 1.24 Ma [*Berggren et al.*, 1995; *Raffi et al.*, 2006]. In contrast, no *G. oceanica* and only small-sized *Gephyrocapsa* (<3.5 μm) can be observed on the other side where the Jaramillo normal magnetic event was identified, suggesting that the age is younger than 1.07 Ma in the west of the discontinuity. At site 10 in Section S3, *G. oceanica* reappeared. For more information please refer to Figure 6.

Reticulofenestra pseudoumbilicus and *Sphenolithus abies*, the first occurrence datum of medium-sized *Gephyrocapsa oceanica* (>3.5 μm), and the recurrence datum of medium-sized *Gephyrocapsa oceanica*, which correspond to the ages of 3.6 Ma, 1.7 Ma, and 1.04 Ma, respectively [*Berggren et al.*, 1995; *Raffi et al.*, 2006]. In addition, three reversal boundaries of magnetostratigraphy were recognized in Section S3, which are the top of Olduvai (1.77 Ma), the top of Jaramillo (0.99 Ma), and the

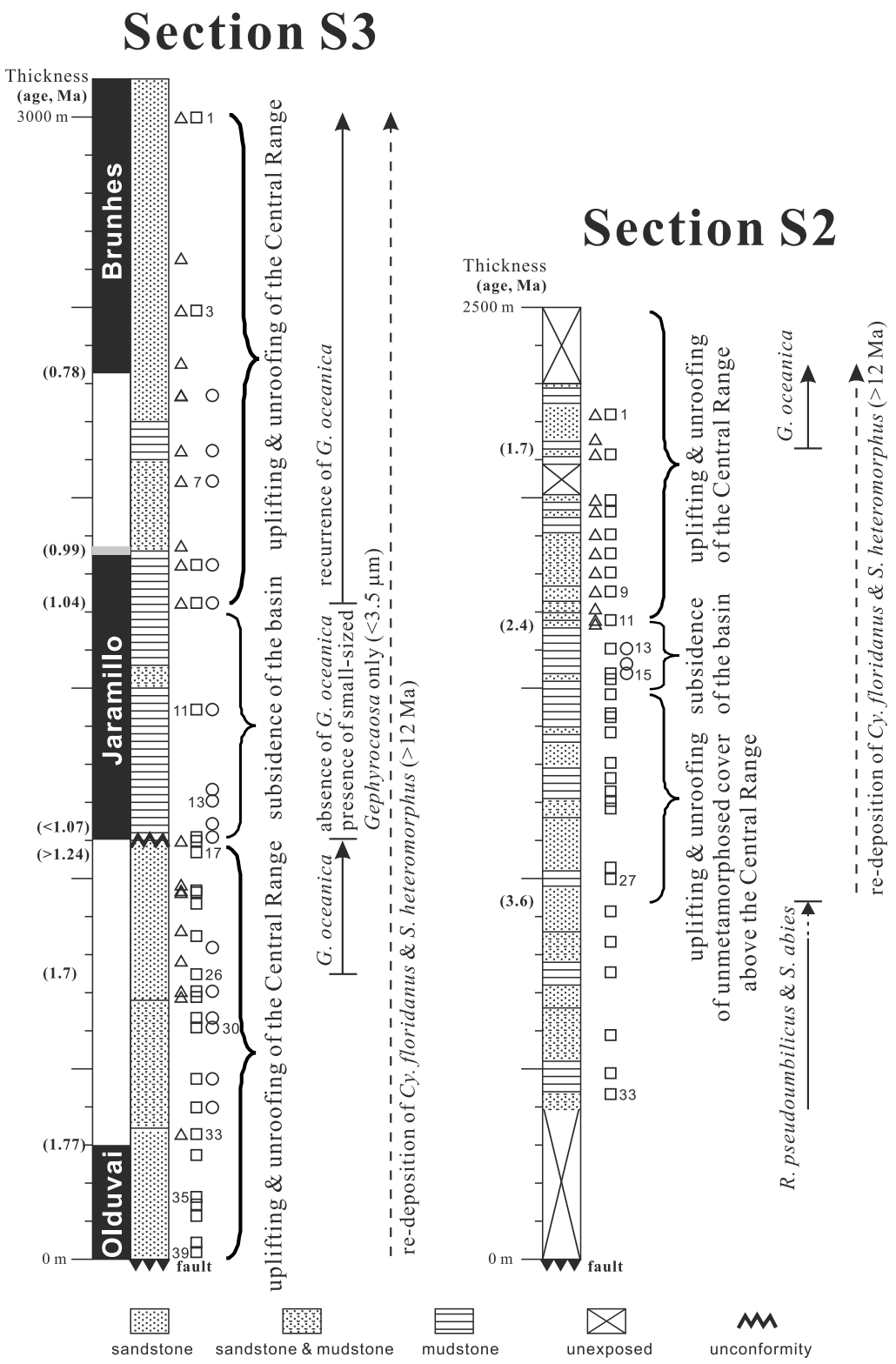

Figure 6. Stratigraphic profiles of magnetic mineral assemblages (Δ: pyrrhotite; □: magnetite; ○: greigite) and magneto-biostratigraphy for two sedimentary sections (S2 and S3) in southwestern Taiwan. Magnetic mineral data and chronology are summarized from this and previous studies [*Chen et al.*, 2001]. It is noted that the age of the first occurrence of detrital pyrrhotite eroded from the Central Range is estimated to be ~2.4 Ma. According to these results, tectonic events including uplifting and unroofing of the Taiwan orogen and subsidence of the surrounding foreland basin are inferred.

base of Brunhes (0.78 Ma). Older nannofossils, such as *Cyclicargolithus floridanus* and *Sphenolithus heteromorphus* (with last occurrence datums at ~12–13 Ma [*Raffi et al.*, 2006]), were sporadically found in the strata younger than 3.6 Ma, indicating that these species were derived from pre-middle Miocene sedimentary strata elsewhere and re-deposited in the ancient foreland basin in southwestern Taiwan. All these chronological data and results of magnetic mineral analysis are summarized in Figure 6 as a stratigraphic profile for each of Sections 2 and 3.

[14] The magnetic mineral assemblages shown in Figure 6 are fairly complicated. In addition to magnetite, pyrrhotite and greigite (Fe_3S_4) also appear in the two sections which reveal that pyrrhotite is preferentially present in sandy or silty layers, showing further evidence for its detrital origin. Based on the two datum events of nannofossils (*i.e.*, the last occurrence of *R. pseudoumbilicus* and *S. abies* at 3.6 Ma and the first occurrence of medium-sized *G. oceanica* at 1.7 Ma) and their stratigraphic positions (Figure 6), the age for the first occurrence of detrital pyrrhotite (located at site 12 of Section S2) is estimated to be ~2.4 Ma. By contrast, greigite is prevalent in fine-grained layers, particularly in massive and thick mudstones (i.e., sites 13–15 of Section S2 and sites 9–15 of Section S3 in Figure 6). Greigite has been regarded as a diagenetic product [*Horng et al.*, 1992; *Roberts et al.*, 2011], and it is widespread in muddy sediments off southwestern Taiwan at water depths over 500 m [*Horng and Chen*, 2006]. Therefore, the sedimentary environment of the thick, greigite-bearing mudstones in Sections 2 and 3 must be deeper than that of the sandy layers, suggesting subsidence in the ancient foreland basin.

[15] Associated with subsidence of the basin is uplifting and subsequent unroofing of the Central Range. Based on the changes in magnetic mineral and lithology of the sections (Figure 6), we propose that these tectonic processes might happen episodically since the late Pliocene. As evidenced by the simple magnetic composition (i.e., magnetite) and re-deposition of pre-middle Miocene (>12 Ma) calcareous nannofossils (e.g., *Cy. floridanus* and *S. heteromorphus*) in the basin, the first episodic event started at 3.6 Ma, which indicates an early uplifting and unroofing of unmetamorphosed sedimentary rocks that lay above the pyrrhotite-bearing metamorphic terranes. It was not until around 2.4 Ma that a subsidence of the basin occurred and caused the formation of greigite in a deep-water environment. Followed by this event is another exhumation of the Central Range, which resulted in the onset of denudation of pyrrhotite-bearing metamorphic terranes. Since then, detrital pyrrhotite was deposited rather continuously in the basin until another subsidence occurred during the ages of <1.07–1.04 Ma. After 1.04 Ma, another episode of uplifting of the Central Range caused metamorphic pyrrhotite to be eroded to the basin again. The high sedimentation rates in the ancient foreland basin (from 650 m/m.y. (3.6–1.7 Ma) to 2100 m/m.y. (1.77–0.78 Ma)) indicate that exhumation and denudation of Taiwan's Central Range must have accelerated since the late Pliocene.

8. Conclusions

[16] Our work has demonstrated that pyrrhotite is a characteristic magnetic mineral in the epizone and greenschist facies of Taiwan's young orogen. Formed in the outer part of the orogen by low-grade regional metamorphism, pyrrhotite can be used as a tracer to unravel the early history of the orogen's exhumation and denudation. Our study indicates that pyrrhotite is probably more common than previously thought in low-grade metamorphic orogens and their surrounding basins. We suggest that pyrrhotite may find a wider application as a provenance tracer for sediments sourced from orogens with high uplift and denudation rates like Taiwan.

Acknowledgments

[17] We thank Wei Lo, Ping-Ru Huang, Kung-Liang Lai, Te-Cheng Yi, Hsien-Neng Hu, and Wei-Hao Hsu for help with collecting samples for this work. We are grateful to Andrew Roberts, Fabio Florindo and Editors for their constructive comments and help in improving the manuscript. This study is supported by the Institute of Earth Sciences, Academia Sinica, and National Science Council grants NSC100-2116-M-001-016 (to CSH) and NSC100-2611-M-001-002 (to CAH).

References

Berggren, W. A., F. J. Hilgen, C. G. Langereis, D. V. Kent, J. D. Obradovich, I. Raffi, M. E. Raymo, and N. J. Shackleton (1995), Late Neogene chronology: New perspectives in high-resolution stratigraphy, *Geol. Soc. Am. Bull.*, *107*, 1272–1287, doi:10.1130/0016-7606(1995)107<1272:LNCNPI>2.3.CO;2.

Beyssac, O., M. Simoes, J. P. Avouac, K. A. Farley, Y. G. Chen, Y. C. Chan, and B. Goffé (2007), Late Cenozoic metamorphic evolution and exhumation of Taiwan, *Tectonics*, *26*, TC6001, doi:10.1029/2006TC002064.

Carpenter, R. H. (1974), Pyrrhotite isograd in southeastern Tennessee and southwestern North Carolina, *Geol. Soc. Am. Bull.*, *85*, 451–456, doi:10.1130/0016–7606(1974)85<451:PIISTA>2.0.CO;2.

Chen, C. H., and C. H. Wang (1995), *Explanatory Notes for the Metamorphic Facies Map of Taiwan*, 2nd Ed., 51 pp., Cent. Geol. Surv., Taipei.

Chen, W. S., K. D. Ridgway, C. S. Horng, Y. G. Chen, K. S. Shea, and M. G. Yeh (2001), Stratigraphic architecture, magnetostratigraphy, and incised-valley systems of the Pliocene-Pleistocene collisional marine foreland basin of Taiwan, *Geol. Soc. Am. Bull.*, *113*, 1249–1271, doi:10.1130/0016-7606(2001)113<1249:SAMAIV>2.0.CO;2.

Dadson, S. J., et al. (2003), Links between erosion, runoff variability and seismicity in the Taiwan orogeny, *Nature*, *426*, 648–651, doi:10.1038/nature02150.

Evans, M. E., and F. Heller (2003), *Environmental Magnetism: Principles and Applications of Enviromagnetics*, 299 pp., Academic, San Diego, Calif.

Graham, A. R. (1969), Quantitative determination of hexagonal and monoclinic pyrrhotites by X-ray diffraction, *Can. Mineral.*, *10*, 4–24.

Griffiths, G. A. (1979), High sediment yields from major rivers of the Western Southern Alps, New Zealand, *Nature*, *282*, 61–63, doi:10.1038/282061a0.

Ho, C. S. (1975), *An introduction to the geology of Taiwan: Explanatory text of the geologic map of Taiwan*, 153 pp., Minist. of Econ. Aff., Taipei.

Horng, C. S., and K. H. Chen (2006), Complicated magnetic mineral assemblages in marine sediments offshore of southwestern Taiwan: Possible influence of methane flux on the early diagenetic process, *Terr. Atmos. Ocean. Sci.*, *17*, 1009–1026.

Horng, C. S., and C. A. Huh (2011), Magnetic properties as tracers for source-to-sink dispersal of sediments: A case study in the Taiwan Strait, *Earth Planet. Sci. Lett.*, *309*, 141–152, doi:10.1016/j.epsl.2011.07.002.

Horng, C. S., and A. P. Roberts (2006), Authigenic or detrital origin of pyrrhotite in sediments?: Resolving a paleomagnetic conundrum, *Earth Planet. Sci. Lett.*, *241*, 750–762, doi:10.1016/j.epsl.2005.11.008.

Horng, C. S., J. C. Chen, and T. Q. Lee (1992), Variations in magnetic minerals from two Plio-Pleistocene marine-deposited sections, southwestern Taiwan, *J. Geol. Soc. China*, *35*, 323–335.

Horng, C. S., M. Torii, K. S. Shea, and S. J. Kao (1998), Inconsistent magnetic polarities between greigite- and pyrrhotite/magnetite-bearing marine sediments from the Tsailiao-chi section, southwestern Taiwan, *Earth Planet. Sci. Lett.*, *164*, 467–481.

Itaya, T. (1975), Pyrrhotite from the Sanbagawa politic schists of the Shiraga-yama area, central Shikoku, Japan, *Mineral. J.*, *8*, 25–37, doi:10.2465/minerj.8.25.

Li, Y. H. (1976), Denudation of Taiwan Island since the Pliocene epoch, *Geology*, *4*, 105–107, doi:10.1130/0091-7613(1976)4<105:DOTIST>2.0.CO;2.

Ludwig, W., and J. L. Probst (1998), River sediment discharge to the oceans: Present-day controls and global budgets, *Am. J. Sci.*, *298*, 265–295, doi:10.2475/ajs.298.4.265.

Milliman, J. D., and R. H. Meade (1983), World-wide delivery of river sediment to the oceans, *J. Geol.*, *91*, 1–21, doi:10.1086/628741.

Milliman, J. D., and J. P. M. Syvitski (1992), Geomorphic/tectonic control of sediment discharge to the ocean: The importance of small mountainous rivers, *J. Geol.*, *100*, 525–544, doi:10.1086/629606.

Raffi, I., J. Backman, E. Fornaciari, H. Pälike, D. Rio, L. Lourens, and F. Hilgen (2006), A review of calcareous nannofossil astrobiochronology encompassing the past 25 million years, *Quat. Sci. Rev.*, *25*, 3113–3137, doi:10/1016/j.quascirev.2006.07.007.

Roberts, A. P., L. Chang, C. J. Rowan, C. S. Horng, and F. Florindo (2011), Magnetic properties of sedimentary greigite (Fe_3S_4): An update, *Rev. Geophys.*, *49*, RG1002, doi:10.1029/2010RG000336.

Rochette, P. (1987), Metamorphic control of the magnetic mineralogy of black shales in the Swiss Alps: Toward the use of "magnetic isograde", *Earth Planet. Sci. Lett.*, *84*, 446–456, doi:10.1016/0012-821X(87)90009-4.

Yui, T. F. (2005), Isotopic composition of carbonaceous material in metamorphic rocks from the mountain belt of Taiwan, *Int. Geol. Rev.*, *47*, 310–325, doi:10.2747/0020-6814.47.3.310.